

# Recurrent *EWSR1-CREB3L1* Gene Fusions in Sclerosing Epithelioid Fibrosarcoma

Elsa Arbajian, MSc,\* Florian Puls, MD, FRCPath,† Linda Magnusson, MSc,\*  
 Khin Thway, BSc, MBBS, FRCPath,‡ Cyril Fisher, MD, DSc, FRCPath,‡  
 Vaiyapuri P. Sumathi, MD, FRCPath,† Johnbosco Tayebwa, MSc,\* Karolin H. Nord, PhD,\*  
 Lars-Gunnar Kindblom, MD, PhD,† and Fredrik Mertens, MD, PhD\*

**Abstract:** Sclerosing epithelioid fibrosarcoma (SEF) and low-grade fibromyxoid sarcoma (LGFMS) are 2 distinct types of sarcoma, with a subset of cases showing overlapping morphologic and immunohistochemical features. LGFMS is characterized by expression of the MUC4 protein, and about 90% of cases display a distinctive *FUS-CREB3L2* gene fusion. In addition, SEF is often MUC4 positive, but is genetically less well studied. Fluorescence in situ hybridization (FISH) studies have shown involvement of the *FUS* gene in the majority of so-called hybrid LGFMS/SEF and in 10% to 25% of sarcomas with pure SEF morphology. In this study, we investigated a series of 10 primary tumors showing pure SEF morphology, 4 cases of LGFMS that at local or distant relapse showed predominant SEF morphology, and 1 primary hybrid LGFMS/SEF. All but 1 case showed diffuse expression for MUC4. Using FISH, reverse transcription polymerase chain reaction, and/or mRNA sequencing in selected cases, we found recurrent *EWSR1-CREB3L1* fusion transcripts by reverse transcription polymerase chain reaction in 3/10 pure SEF cases and splits and deletions of the *EWSR1* and/or *CREB3L1* genes by FISH in 6 additional cases. All 5 cases of LGFMS with progression to SEF morphology or hybrid features had *FUS-CREB3L2* fusion transcripts. Our results indicate that *EWSR1* and *CREB3L1* rearrangements are predominant over *FUS* and *CREB3L2* rearrangements in pure

SEF, highlighting that SEF and LGFMS are different tumor types, with different impacts on patient outcome.

**Key Words:** sclerosing epithelioid fibrosarcoma, low-grade fibromyxoid sarcoma, hybrid, gene fusion, *EWSR1*, *FUS*, *CREB3L1*, *CREB3L2*

(*Am J Surg Pathol* 2014;38:801–808)

Sclerosing epithelioid fibrosarcoma (SEF) is a rare type of sarcoma characterized by a proliferation of epithelioid cells arranged in nests and cords in a distinctly sclerotic hyalinized stroma. It is most often found in the deep musculature of the lower extremities, although a wide spectrum of locations has been described.<sup>1</sup> SEF is highly malignant, recurring locally in more than half of the patients and with a metastasis rate of 40% to 80%; according to the 2 largest series published, 25% to 57% of the patients die from their disease.<sup>2,3</sup> Morphologically, SEF can mimic myoepithelioma, carcinoma with desmoplastic stroma, or, to a lesser extent, sclerosing lymphoma, synovial sarcoma, or other malignant fibroblastic proliferations. Recognition of SEF is therefore important for adequate patient management.

Previous studies of SEF have noted that some cases show areas reminiscent of low-grade fibromyxoid sarcoma (LGFMS), suggesting a biological relationship between the 2 sarcoma types.<sup>4–7</sup> LGFMS is a distinctive, low-grade malignant fibroblastic tumor with much lower potential for recurrence and metastasis than SEF; it could be noted, however, that late metastases might be more common than initially suspected.<sup>8,9</sup> Expression of the MUC4 protein is a consistent finding at immunohistochemical (IHC) analysis of LGFMS, but is seen also in about 70% of SEF cases.<sup>1</sup> The vast majority of LGFMS shows a characteristic translocation t(7;16) that results in the *FUS-CREB3L2* gene fusion; a few cases instead display an *FUS-CREB3L1* fusion,<sup>10</sup> and, recently, Lau et al<sup>11</sup> reported an *EWSR1-CREB3L1* fusion in 2 cases. Areas morphologically indistinguishable from SEF have been identified in primary LGFMS. In addition, recurrences or metastases of LGFMS may uniformly or partly show SEF morphology.<sup>5,7,8,12</sup> The impact on clinical behavior for these tumors with hybrid features (hereafter referred to as hybrid

From the \*Department of Clinical Genetics, University and Regional Laboratories, Skåne University Hospital, Lund University, Lund, Sweden; †Department of Musculoskeletal Pathology and Orthopaedic Oncology, Royal Orthopaedic Hospital NHS Foundation Trust and Division of Cancer Studies, Medical School, University of Birmingham, Birmingham; and ‡Department of Histopathology, Royal Marsden Hospital, London, UK.

Conflicts of Interest and Source of Funding: Supported by grants from the Swedish Cancer Society, the Swedish Research Council, the Inga Britt and Arne Lundberg Foundation, and the Medical Faculty of Lund University. The authors have disclosed that they have no significant relationships with, or financial interest in, any commercial companies pertaining to this article.

Correspondence: Elsa Arbajian, MSc, Department of Clinical Genetics, University Hospital, SE-221 85 Lund, Sweden (e-mail: elsa.arbajian@med.lu.se).

Supplemental Digital Content is available for this article. Direct URL citations appear in the printed text and are provided in the HTML and PDF versions of this article on the journal's Website, www.ajsp.com.

Copyright © 2014 by Lippincott Williams & Wilkins

LGFMS-SEF)<sup>12</sup> in comparison with tumors displaying uniform SEF or LGFMS morphology (hereafter referred to as pure SEF or pure LGFMS) remains unclear.

Genetic analyses of SEF have shown that hybrid tumors displaying both LGFMS-like and SEF-like features often display the same gene fusions as in pure LGFMS.<sup>5-7,12,13</sup> Limited studies on pure SEF tumors that do not display any LGFMS-like areas have shown that *FUS* rearrangements occur in this subtype as well but seemingly at a much lower frequency.<sup>14,15</sup> In this study, we report recurrent *EWSR1-CREB3L1* fusions in a series of pure SEF and *FUS-CREB3L2* fusions in LGFMS that relapsed with SEF-like morphology or that showed hybrid LGFMS/SEF morphology in the primary lesion.

## MATERIALS AND METHODS

### Patients and Tumors

The present study included 10 primary SEFs (cases 1 to 10), 4 cases of LGFMS that recurred with SEF morphology (cases 11 to 14), and 1 primary hybrid LGFMS/SEF (case 15; Table 1). Fresh tumor biopsies were available from cases 1 to 4. Cut sections from paraffin-embedded tumors were available from cases 5 to 15. All cases were retrieved from the Department of Musculoskeletal Pathology at the Royal Orthopedic Hospital, Birmingham, UK. Sample collection, analyses, and data collection were performed in agreement with the local ethical guidelines.

### IHC for MUC4

Paraffin wax sections were cut at 2  $\mu$ m, dried on and antigen retrieved in epitope retrieval solution pH8 (RE7116; Novocastra, Newcastle, UK) at 68°C for 17 hours in a stirred water bath. The rabbit polyclonal anti-human MUC4 antibody (Santa Cruz Biotechnology, Heidelberg, Germany) was used in 1:200 dilution with an LGFMS as positive control. The DakoCytomation En-Vision Detection System peroxidase/DAB visualization (K5007; Dako, Ely, UK) was used according to the manufacturer's instructions.

### mRNA Sequencing and Data Analysis

mRNA libraries were prepared from case 3 for sequencing using the Truseq RNA sample preparation kit v2 (Illumina) according to the manufacturer's protocol. In brief, 200 to 1000 ng of total RNA was enriched for poly-A tailed RNA using magnetic oligo-dT beads. The poly-A tailed enriched RNA was fragmented to a median size of 400 nucleotides by thermal fragmentation at 94°C for 10 seconds in the "Elute, Prime, Fragment" buffer. The fragmented RNA was used as templates for cDNA synthesis using Superscript II reverse transcriptase (Invitrogen, Carlsbad, CA). A second DNA strand was produced using DNA polymerase I and RNase H. After end repair and 3' end-adenylation, indexed adapters were ligated to the double-stranded cDNA fragments. The adapter-bound fragments were then enriched using a 15-

cycle polymerase chain reaction (PCR). Paired-end 101 bp reads were generated from the cDNA libraries using a HiscanSQ (Illumina).

To identify fusion transcripts using paired-end RNA-Seq data, analyses were performed on gzip-compressed fastq files using TopHat2.0.7 with the *-fusion-search* and *-bowtie1* options, only allowing for detection of fusions within a minimum distance of 100,000 bp (*-fusion-min-dist* option). UCSC hg19 was used as the human genome reference. The fragment length of the data ranged from 100 to 1000 bp with a mean of 400 bp so the mate inner distance (*-r* option) was set to 200 with an SD (*-mate-std-dev* option) of 200. TopHat-fusion-post was run on the output files from TopHat2.0.7 to filter for fusions with at least 1 fusion-spanning read and 2 fusion-spanning mate-pairs.<sup>16</sup>

### Reverse Transcription PCR Analyses

#### Reverse Transcription PCR for the *EWSR1-CREB3L1* Gene Fusion

Total RNA was extracted from frozen tumor tissue from cases 1 to 4 using the RNeasy Lipid Tissue Mini Kit following the manufacturer's instructions (Qiagen, Valencia, CA). RNA (2.5  $\mu$ g) was mixed with random hexamers at an end concentration of 43  $\mu$ M and RNase-free H<sub>2</sub>O up to a volume of 11.5  $\mu$ L. The mix was incubated for 5 minutes at 65°C, followed by 1 minute at 4°C. In parallel, a mix of total volume of 8.5  $\mu$ L of 1  $\times$  FSB, 10 mM DTT, 0.5 mM dNTPs in DEPC water, 2 U RNase inhibitor (Promega, WI) and 200 U MMLV was prepared and added to the RNA mix. cDNA was synthesized by incubating this mix for 1 hour at 37°C, followed by 5 minutes at 65°C. Forward and reverse primers specific for *EWSR1* and *CREB3L1*, respectively, were designed to detect possible fusion transcripts. PCR reactions were performed in a 50  $\mu$ L total reaction volume containing 1  $\times$  PCR buffer, 1 mM dNTPs, 1.25 mM MgCl<sub>2</sub>, 0.5  $\mu$ M of each of the forward and reverse primers, 1 U Taq Polymerase (Invitrogen), and 1  $\mu$ L cDNA template. Details about primers and PCR cycles can be found in Supplementary Table 1 (Supplemental Digital Content 1, <http://links.lww.com/PAS/A189>). Amplified fragments were purified from agarose gels and directly sequenced using the Big Dye v1.1 cycle sequencing kit (Applied Biosystems, Foster City) on an ABI-3100 Avant genetic analyzer (Applied Biosystems). Obtained sequence data were then analyzed using the BLASTN software (<http://blast.ncbi.nlm.nih.gov/Blast.cgi>).

#### Reverse Transcription PCR for the *FUS-CREB3L2* Gene Fusion

RNA was extracted from blocks of formalin-fixed paraffin-embedded tissue from cases 11 to 15 as described.<sup>17</sup> Primer pairs for reverse transcription PCR (RT-PCR) located in *FUS* exons 5, 6, and 9 and *CREB3L2* exons 5 and 6 were used as described by Guillou et al.<sup>5</sup> All primers were purchased from Eurofins MWG Operon-Biotech (Ebersberg, Germany). RT-PCR

**TABLE 1.** Clinical Data on 15 Patients With Pure SEF or Hybrid LGFMS/SEF Morphology

Case	Age/Sex	Size*	Location (Morphology)	Relapse (mo)†	MUC4‡	Follow-up§
1	74/M	16 (NR)	Chest wall (SEF)	Lung met (0)	Positive	15 DOD
2	60/M	Unknown (NR)	Groin (SEF)	Lung and bone met (0)	Positive	4 DOD
3	51/F	13 (NR)	Pelvis (SEF)	Unknown	Positive	39 DOD
4	42/F	10	Shoulder (SEF)	Lung (9) and bone (25) met	Positive	53 DOD
5	47/M	Unknown	L leg (SEF)	Lymph node and lung met (6)	Positive	75 DOD
6	52/M	10	Chest wall (SEF)	None	Positive	46 LTF
7	46/F	9.5	Knee (SEF)	Bone met (13)	Positive	29 DOD
8	41/F	9	Kidney (SEF)	Bone (0) and lung (5) met	Positive	22 DOD
9	28/M	Unknown	Paraspinal (SEF)	Bone met (6)	Positive	32 DOD
10	91/F	Unknown	Finger (SEF)	None	Negative	80 DOUC
11	45/M	17	Thigh (LGFMS)	Chest wall met (5)	Positive	55 DOD
12	42/F	Unknown	Chest wall met (SEF) Thigh (LGFMS)	Lung met (4)	Positive	43 DOD
13	22/M	Unknown	Lung met (SEF) Shoulder (LGFMS?) LR (SEF) Thigh met (SEF)	LR (360, 466, 533) Soft tissue met (610)	Positive	610 AWD
14	53/F	4	Buttock (LGFMS) LR (LGFMS/SEF)	LR (56) Lung met (96)	Positive	151 AWD
15	49/M	6	Abdominal wall (LGFMS/SEF)	None	Positive	6 NED

\*Largest diameter in centimeters. For nonresected (NR) lesions, largest radiologic diameter is given.

†Time to relapse in months after diagnosis.

‡IHC for MUC4 expression.

§Follow-up is given in months from diagnosis.

AWD indicates alive with disease; DOD, dead of disease; DOUC, dead of unknown causes; L leg, lower leg; LR, local recurrence; LTF, lost to follow-up; met, metastasis; NED, no evidence of disease.

reactions were performed with the OneStep RT-PCR kit (Qiagen, Hilden, Germany) and were run for 40 cycles. Reaction products were visualized in 10% polyacrylamide gel after electrophoresis. PCR products were Sanger sequenced at the Functional Genomics Laboratory at Birmingham University using a 3700 DNA Analyser (Applied Biosystems, Warrington, UK).

### Fluorescence In Situ Hybridization Analyses

Interphase nuclei from cases 1 to 10 were studied with regard to rearrangement of the *FUS* (16p11), *EWSR1* (22q12), *CREB3L1* (11p11), *CREB3L2* (7q34), and *MDM2* (12q15) genes, using BAC probes detailed in Supplementary Table 2 (Supplemental Digital Content 2, <http://links.lww.com/PAS/A190>). The BAC clones were selected on the basis of their location in the UCSC Human Genome Browser Gateway (<http://genome.ucsc.edu/cgi-bin/hgGateway>, hg19) and obtained from the BACPAC Resource Center (<http://bacpac.chori.org>). Except for the *MDM2* gene, all probe sets flanked the genes and were used as break-apart probes. Probe preparation, hybridization, and analysis were performed as previously described.<sup>18</sup> The cutoff level for scoring aberrations was 30% abnormal nuclei.

## RESULTS

### Morphology and IHC

Cases 1 to 10 showed uniform pure SEF morphology with moderate to high cellularity. The tumors were composed of small to medium-sized plump to epithelioid cells with a small rim of distinct clear cytoplasm. The cells were

embedded within a densely sclerotic matrix. Nuclei were oval to slightly elongate with finely speckled chromatin (Fig. 1). All but 1 tumor (case 10) showed expression of MUC4 at IHC analysis. Focal chondroid differentiation was noted in 1 tumor (case 7; Figs. 1E, F). No expression for S100 (except for the chondroid area of case 7), cytokeratins (AE1/AE3), desmin, or CD45 was identified (data not shown). Clinical workup showed that 2 tumors (cases 11 and 12) were in fact metastases of primary tumors with LGFMS morphology (Figs. 2A, B). Two tumors (cases 13 and 14) were local recurrences. A primary LGFMS was confirmed in case 14. In case 13 (Fig. 2D), a tumor at the same location had been excised 30 years previously (in 1962). From this resection only a paper copy of the report was available: “*The microscopic features of this lesion consist of fibres and elongated wavy nuclei arranged mainly in parallel rows in an oedematous matrix, with an occasional whorled area and areas where the fibre bundles are cut transversely. This is the picture of neurofibroma.*” Misinterpretation as neurofibroma is a well-recognized diagnostic pitfall, and LGFMS was not identified as an entity until 1987.<sup>19</sup> One tumor (case 15) showed features of an LGFMS with abrupt transition to a high-grade sarcoma with densely packed epithelioid cells. MUC4 expression was identified in both components (Fig. 2C).

### EWSR1-CREB3L1 Gene Fusions

RNA sequencing of case 3 showed 46 fusion-spanning reads and 20 fusion-spanning mate-pairs supporting an *EWSR1-CREB3L1* fusion transcript. RT-PCR for *EWSR1-CREB3L1* fusion transcripts in this and 3 other primary pure SEFs from which frozen tumor samples were available (cases

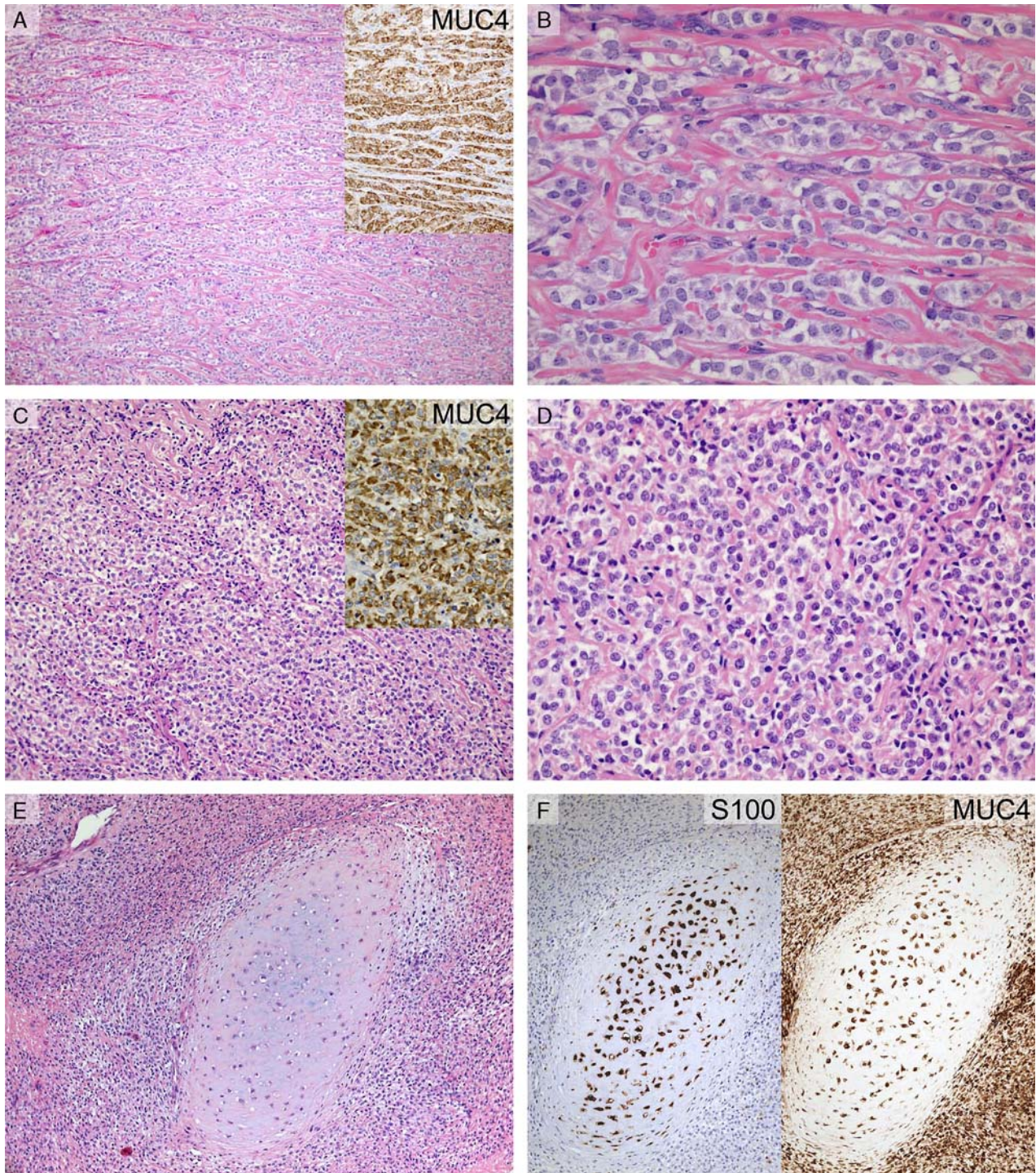


**FIGURE 1.** Morphologic and IHC features of sarcomas with pure SEF morphology. A and B, Case 9 (*FUS* and *EWSR1* FISH negative) showed medium-sized epithelioid cells situated within a collagenized matrix. There was strong and diffuse cytoplasmic staining for MUC4 (A, inset). C and D, Case 3 (*EWSR1-CREB3L1* fusion positive) showed an identical morphology and staining for MUC4 (C, inset). E and F, Case 7 (loss of 5'-part of *CREB3L1* and hemizygous deletion of *FUS* and *EWSR1*) showed foci of cartilaginous differentiation highlighted by S100 (F, left). MUC4 expression was retained within the cartilaginous focus (F, right).

1 to 4) detected in-frame fusions in 3 of them (cases 2 to 4), joining different exons of *EWSR1* (exons 11, 8, or 7, respectively) to exon 6 of *CREB3L1* (Fig. 3).

To search for further gene fusion–positive cases, interphase fluorescence in situ hybridization (FISH) was performed on the 10 primary SEFs (cases 1 to 10) using

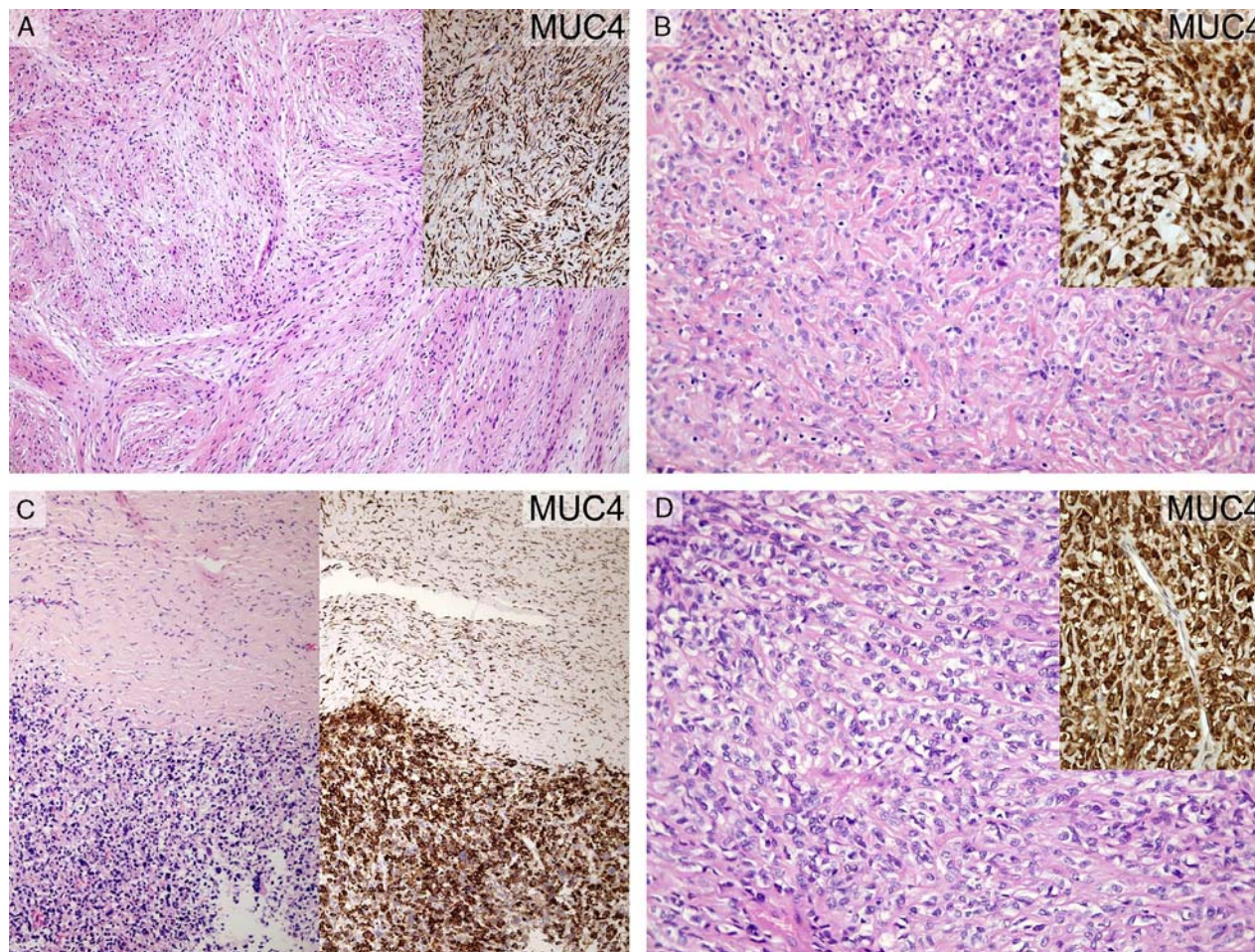


**FIGURE 2.** Morphologic and IHC features of sarcomas with hybrid LGFMS/SEF morphology (all *FUS-CREB3L2* fusion positive). Case 11 presented with a soft tissue metastasis displaying SEF morphology (B) 5 months after an LGFMS had been excised (A). C, Case 15 showed abrupt transition from LGFMS to SEF within the primary lesion. D, Case 13 presented with a tumor with SEF morphology; however, a tumor compatible with LGFMS had been excised at the same site 30 years earlier. Staining for MUC4 is shown in insets.

break-apart probes for *EWSR1* and *FUS* (potential 5'-partners), as well as *CREB3L1* and *CREB3L2* (potential 3'-partners). In addition, the status of the *MDM2* gene was investigated, as one previously reported SEF had amplification of this gene.<sup>20</sup> The results are summarized in Table 2. In brief, split signals or loss of the part flanking the 3'-part of the gene, indicative of involvement in a gene fusion, were seen in 5/10 informative cases for the *EWSR1* gene, with another 3 cases showing hemizygous deletion. None of the cases had any structural *FUS* rearrangement, but a hemizygous deletion was found in 1/7 informative cases. The *CREB3L1* gene showed split signals or loss of the part covering the 5'-part of the locus in 5/7 cases. In 3 of the *CREB3L1*-positive SEFs (cases 1, 3, and 4), the *EWSR1* locus was also rearranged (Fig. 3). The other 2 showed either hemizygous deletion of both *EWSR1* and *FUS* (case 7) or of only *EWSR1* (case 10). FISH for *CREB3L2* was negative in 5/5 cases. None of 8 informative cases showed amplification of *MDM2*.

### *FUS-CREB3L2* Gene Fusions

All 4 tumors (cases 11 to 14) with a morphology compatible with LGFMS in the primary lesion and with SEF at relapse, as well as the primary hybrid LGFMS/SEF (case 15), displayed *FUS-CREB3L2* fusion transcripts, joining different exons of *FUS* (exons 6 or 8) to exon 5 of *CREB3L2*.

### DISCUSSION

The vast majority (> 90%) of LGFMS displays an *FUS-CREB3L2* chimera. Negative tumors instead harbor an *FUS-CREB3L1* fusion,<sup>10</sup> or the recently described *EWSR1-CREB3L1* fusion.<sup>11</sup> In contrast to the marked predominance of *FUS-CREB3L2* in LGFMS, the genetics of SEF seems more heterogenous. Previous cytogenetic information on SEF, including pure and so-called hybrid cases of LGFMS/SEF, is limited to the findings of a 12q amplification in 1 case,<sup>20</sup> 10p11 rearrangements in 2 cases,<sup>20,21</sup> and the t(7;16) in 1 case.<sup>12</sup> In addition, FISH

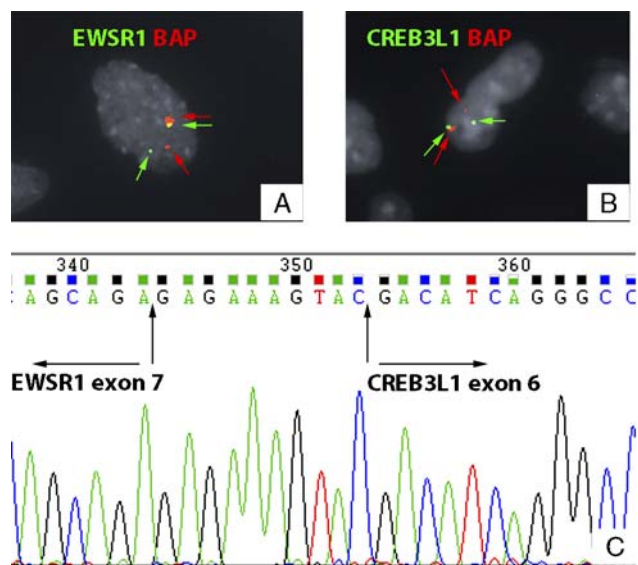


**FIGURE 3.** Genetic findings in pure SEFs. A, Interphase FISH showing split signals with a break-apart probe for the *EWSR1* gene in case 4. B, Interphase FISH showing split signals with a break-apart probe for the *CREB3L1* gene in case 3. C, Chromatogram of the fragment obtained by RT-PCR in case 4 with a forward primer for *EWSR1* and a reverse primer for *CREB3L1*. The fusion was between *EWSR1* exon 7 and *CREB3L1* exon 6, with a 10 bp insert at the fusion point.

studies of hybrid LGFMS/SEF tumors have shown frequent involvement of the *FUS* gene.<sup>5-7,13</sup> Much less genetic information is available for pure SEF, but 2 recent interphase FISH studies identified *FUS* rearrangements in 2/22 (9%) and 6/23 (26%) cases, respectively.<sup>12,14</sup> The study by Doyle et al<sup>12</sup> included data also on MUC4 immunostatus: 6/15 MUC4-positive tumors, but none of 8 MUC4-negative SEFs, had an *FUS* rearrangement. Doyle and colleagues also used interphase FISH to study

the status of the *EWSR1*, *CREB3L1*, and *CREB3L2* genes in a small number of MUC4-positive cases: 0/1, 1/3, and 1/2 cases, respectively, were positive. The *CREB3L1*-positive and *CREB3L2*-positive cases concomitantly showed *FUS* rearrangements, suggesting the existence of an *FUS-CREB3L1* or *FUS-CREB3L2* fusion in a subset of pure SEF. Furthermore, 2/3 MUC4-positive hybrid LGFMS/SEF tumors showed FISH results indicative of an *EWSR1-CREB3L1* fusion.<sup>12</sup>

The present study comprised 15 tumors with SEF morphology, either uniformly (so-called pure SEF, 10 cases) or in synchronous (so-called hybrid LGFMS/SEF) or metachronous combination with LGFMS morphology (5 cases). All hybrid LGFMS/SEF cases had *FUS-CREB3L2* fusion transcripts, whereas none of the 10 pure SEFs showed evidence of *FUS* rearrangement. Fourteen tumors were MUC4 positive. Although the frequency of MUC4 positivity was slightly higher than that of Doyle and colleagues (14/15 vs. 20/29), the frequency of *FUS* rearrangements was similar (5/15 vs. 6/23). Wang et al<sup>14</sup> reported *FUS* rearrangements in 2/22 SEFs. The variation among the 3 series might in part be attributed to the fact that they were all relatively small but also to different definitions of SEF. In our series, 4/5 cases with *FUS-CREB3L2* fusions were local recurrences or metastases of LGFMS, and the remaining case was a hybrid LGFMS/SEF. A shift of the prevailing morphologic pattern from LGFMS to SEF in local recurrences/metastases has been previously described.<sup>22</sup> The clinical significance of this morphologic progression, or of the presence of focal SEF-like areas in LGFMS, is uncertain.

In 4/10 tumors with pure SEF morphology (cases 1 to 4), an *EWSR1-CREB3L1* fusion was detected by FISH, RT-PCR, and/or RNA sequencing techniques. Probably because of technical limitations inherent in the methods used, the results did not always support each other. For example, in case 1, FISH analysis clearly

**TABLE 2.** Results of RT-PCR and FISH Analyses on 10 Cases of Pure SEF and 5 Cases of Hybrid LGFMS/SEF\*

Case	RT-PCR	<i>FUS</i>	<i>EWSR1</i>	<i>CREB3L1</i>	<i>CREB3L2</i>	<i>MDM2</i>
1	ND	Neg	Split	Split	Neg	3 copies
2	<i>EWSR1-CREB3L1</i>	Neg	Neg	ND	ND	Neg
3	<i>EWSR1-CREB3L1</i>	Neg	Del 3'	Split	Neg	Neg
4	<i>EWSR1-CREB3L1</i>	Neg	Split	Split	Neg	ND
5	ND	ND	Del 3'	Neg	ND	ND
6	ND	ND	Hem del	Neg	ND	Neg
7	ND	Hem del	Hem del	Del 5'	Neg	Neg
8	ND	ND	Del 3'	ND	Neg	Neg
9	ND	Neg	Neg	ND	ND	Neg
10	ND	Neg	Hem del	Split	ND	Neg
11	<i>FUS-CREB3L2</i>	ND	ND	ND	ND	ND
12	<i>FUS-CREB3L2</i>	ND	ND	ND	ND	ND
13	<i>FUS-CREB3L2</i>	ND	ND	ND	ND	ND
14	<i>FUS-CREB3L2</i>	ND	ND	ND	ND	ND
15	<i>FUS-CREB3L2</i>	ND	ND	ND	ND	ND

\*Cases 1 to 10 showed pure SEF morphology, whereas cases 11 to 15 showed synchronous or metachronous LGFMS and SEF features. In cases 1 to 4, RT-PCR and interphase FISH were performed on RNA and imprint slides, respectively, from frozen tissue, whereas analyses in cases 5 to 15 were performed on paraffin-embedded tumor tissue.

Del 3' indicates loss of signal corresponding to the 3'-part of the gene; del 5', loss of signal corresponding to the 5'-part of the gene; hem del, hemizygous deletion; ND, not done; neg, negative; split, split signals.

showed split signals for both *EWSR1* and *CREB3L1*, strongly suggesting fusion of these 2 genes, but the fusion transcript could not be amplified by RT-PCR. Vice versa, a fusion transcript was found by RT-PCR in case 2, but FISH failed to detect rearrangement of the *EWSR1* locus. In the remaining 2 tumors (cases 3 and 4), all methods—FISH and RT-PCR in both cases and RNA sequencing in case 3—revealed the presence of an *EWSR1-CREB3L1* fusion. From the other 6 primary pure SEFs (cases 5 to 10) only cut sections from formalin-fixed, paraffin-embedded tumor tissue were available. Hence, only interphase FISH analysis could be performed and was not successful for all probes in all cases. Nevertheless, considering that interphase FISH results on cut sections have limited resolution, the finding of split signals for *CREB3L1* (case 10), or loss of its 5'-part (case 7), in combination with loss of 1 copy of the *EWSR1* locus, in 2 of these cases may indicate the presence of an *EWSR1-CREB3L1* fusion in more than half of pure SEFs. In addition, 1 additional tumor showed split signals for *EWSR1* but was negative for all other genes tested (Table 2).

The recurrent finding of *EWSR1* and *FUS* as alternating 5'-partners in gene fusions in some sarcomas (myxoid liposarcoma, angiomatoid fibrous histiocytoma, and Ewing sarcoma) may suggest that the parts contributed by these genes are functionally redundant.<sup>23,24</sup> Indeed, both *FUS* and *EWSR1* encode RNA binding proteins involved in a wide range of cellular processes. Most notably, they regulate RNA polymerase II transcription by interacting with TFIID or RNA polymerase II subunits,<sup>25,26</sup> or by recruiting activators or repressors to the transcription complex.<sup>27,28</sup> They also function in pre-mRNA splicing,<sup>29,30</sup> in DNA repair and genomic stability,<sup>31–33</sup> and in neuronal pathways.<sup>34–37</sup> Still, the frequencies with which these 2 genes are involved in sarcomas vary considerably. For instance, in myxoid liposarcoma, the *FUS-DDIT3* fusion accounts for >95% of the tumors, whereas *EWSR1-DDIT3* occurs in <5%. In contrast, >90% of angiomatoid fibrous histiocytomas display an *EWSR1-CREB1* fusion, with *EWSR1-ATF1* or *FUS-ATF1* as uncommon variant fusions. In addition, some sarcomas have a gene fusion involving *EWSR1* in >99% of the cases, with exceedingly rare (Ewing sarcoma) or no (eg, clear cell sarcoma, desmoplastic round cell tumor) examples of fusions involving *FUS*. Thus, although no obvious histopathologic or clinical differences have been reported for *EWSR1*-positive and *FUS*-positive myxoid liposarcomas, angiomatoid fibrous histiocytomas, or Ewing sarcomas, the fact that one of these two 5' fusion partners is almost always largely prevalent over the other in a certain tumor type strongly indicates that the effects of 5'-*EWSR1* and 5'-*FUS* are different.

This conclusion is supported by the present and previous findings in LGFMS and SEF. In LGFMS and hybrid LGFMS/SEF, *FUS* rearrangements account for >90% of the fusions, whereas *EWSR1* rearrangements seem distinctly more common in primary pure SEFs. As SEF is decidedly more aggressive than LGFMS, this difference may be clinically important. Although *FUS* and

*EWSR1* rearrangements are nonrandomly associated with LGFMS and SEF, respectively, it must be emphasized that the 3'-partners in the gene fusions show a similar, skewed distribution; whereas *CREB3L2* accounts for most cases of LGFMS and hybrid LGFMS/SEF, *CREB3L1* fusions are found in <10% of LGFMS but were seen in 6/9 informative pure SEFs in the present study. Both *CREB3L1* (aka OASIS) and *CREB3L2* (aka BBF2H7) belong to the OASIS family of endoplasmic stress transducers, and, although they show considerable sequence homology, different cellular effects of the 2 proteins cannot be excluded.<sup>38</sup>

A final aspect to consider when trying to explain the distinct and overlapping genetic features in LGFMS and SEF is the cell(s) of origin for these tumors. In a recent study by Straessler et al,<sup>39</sup> it was shown that conditional expression of the *EWSR1-ATF1* chimera in a mouse model resulted in slightly different tumor phenotypes depending on the cell type, and its differentiation stage, in which the fusion was expressed. Hence, possibly the morphologic spectrum from LGFMS over hybrid LGFMS/SEF to pure SEF could be influenced by the type of cell, and its level of differentiation, in which the fusions occur. In this context, it should also be noted that the present series included 1 MUC4-negative SEF, a subgroup in which no gene rearrangements have been described. This case showed split signals for *CREB3L1* at interphase FISH, but no potential fusion partner was identified. Consistent with the findings by Doyle et al,<sup>12</sup> it did not show any *FUS* rearrangement. Thus, it may well be that MUC4-negative SEFs constitute a separate genetic subgroup, further adding to the nosological complexity of the LGFMS-SEF spectrum of tumors.

## ACKNOWLEDGMENTS

The authors thank Drs D.C. Mangham (The Robert Jones and Agnes Hunt Orthopaedic Hospital, Oswestry, UK), N. Deshmukh (Queen Elizabeth Hospital, Birmingham, UK), P. Shenjere (The Christie Hospital, Manchester, UK), and H.-H. Kreipe (Hannover University Hospital, Hannover, Germany) for contribution of cases. The authors are further indebted to A. Niblett, E. Haywood, and G. Marland (Royal Orthopaedic Hospital, Birmingham, UK) and H. Lilljebjörn and M. Rissler (Lund University Hospital, Lund, Sweden) for excellent technical assistance.

## REFERENCES

1. Kindblom LG, Mertens F, Coindre JM, et al. Sclerosing epithelioid fibrosarcoma. In: Fletcher CDM, Bridge JA, Hogendoorn PCW, et al, eds. *WHO classification of Tumours of Soft Tissue and Bone*. Lyon: IARC Press; 2013:97–98.
2. Meis-Kindblom JM, Kindblom LG, Enzinger FM. Sclerosing epithelioid fibrosarcoma. A variant of fibrosarcoma simulating carcinoma. *Am J Surg Pathol*. 1995;19:979–993.
3. Antonescu CR, Rosenblum MK, Pereira P, et al. Sclerosing epithelioid fibrosarcoma: a study of 16 cases and confirmation of a clinicopathologically distinct tumor. *Am J Surg Pathol*. 2001;25:699–709.
4. Folpe AL, Lane KL, Paull G, et al. Low-grade fibromyxoid sarcoma and hyalinizing spindle cell tumor with giant rosettes: a clinicopathologic study of 73 cases supporting their identity and assessing the impact of high-grade areas. *Am J Surg Pathol*. 2000;24:1353–1360.

5. Guillou L, Benhattar J, Gengler C, et al. Translocation-positive low-grade fibromyxoid sarcoma: clinicopathologic and molecular analysis of a series expanding the morphologic spectrum and suggesting potential relationship to sclerosing epithelioid fibrosarcoma: a study from the French Sarcoma Group. *Am J Surg Pathol*. 2007;31:1387–1402.
6. Lane KL, Shannon RJ, Weiss SW. Hyalinizing spindle cell tumor with giant rosettes: a distinctive tumor closely resembling low-grade fibromyxoid sarcoma. *Am J Surg Pathol*. 1997;21:1481–1488.
7. Rekhi B, Folpe AL, Deshmukh M, et al. Sclerosing epithelioid fibrosarcoma—a report of two cases with cytogenetic analysis of FUS gene rearrangement by FISH technique. *Pathol Oncol Res*. 2011;17:145–148.
8. Evans HL. Low-grade fibromyxoid sarcoma: a report of 12 cases. *Am J Surg Pathol*. 1993;17:595–600.
9. Panagopoulos I, Storlazzi CT, Fletcher CDM, et al. The chimeric FUS/CREB3L2 gene is specific for low-grade fibromyxoid sarcoma. *Genes Chromosomes Cancer*. 2004;40:218–228.
10. Mertens F, Fletcher CDM, Antonescu CR, et al. Clinicopathologic and molecular genetic characterization of low-grade fibromyxoid sarcoma, and cloning of a novel FUS/CREB3L1 fusion gene. *Lab Invest*. 2005;85:408–415.
11. Lau PPL, Lui PCW, Lau GTC, et al. EWSRI-CREB3L1 gene fusion: a novel alternative molecular aberration of low-grade fibromyxoid sarcoma. *Am J Surg Pathol*. 2013;37:734–738.
12. Doyle LA, Wang WL, Dal Cin P, et al. MUC4 is a sensitive and extremely useful marker for sclerosing epithelioid fibrosarcoma: association with FUS gene rearrangement. *Am J Surg Pathol*. 2012;36:1444–1451.
13. Reid R, de Silva MV, Paterson L, et al. Low-grade fibromyxoid sarcoma and hyalinizing spindle cell tumor with giant rosettes share a common t(7;16)(q34;p11) translocation. *Am J Surg Pathol*. 2003;27:1229–1236.
14. Wang WL, Evans HL, Meis JM, et al. FUS rearrangements are rare in “pure” sclerosing epithelioid fibrosarcoma. *Mod Pathol*. 2012;25:846–853.
15. Doyle LA, Möller E, Dal Cin P, et al. MUC4 is a highly sensitive and specific marker for low-grade fibromyxoid sarcoma. *Am J Surg Pathol*. 2011;35:733–741.
16. Kim D, Pertea G, Trapnell C, et al. TopHat2: accurate alignment of transcriptomes in the presence of insertions, deletions and gene fusions. *Genome Biol*. 2013;14:R36.
17. Williams A, Bartle G, Sumathi VP, et al. Detection of ASPL/TFE3 fusion transcripts and the TFE3 antigen in formalin-fixed, paraffin-embedded tissue in a series of 18 cases of alveolar soft part sarcoma: useful diagnostic tools in cases with unusual histological features. *Virchows Arch*. 2011;458:291–300.
18. Jin Y, Möller E, Nord KH, et al. Fusion of the AHRH and NCOA2 genes through a recurrent translocation t(5;8)(p15;q13) in soft tissue angiofibroma results in upregulation of aryl hydrocarbon receptor target genes. *Genes Chromosomes Cancer*. 2012;51:510–520.
19. Evans HL. Low-grade fibromyxoid sarcoma. A report of two metastasizing neoplasms having a deceptively benign appearance. *Am J Clin Pathol*. 1987;88:615–619.
20. Gisselsson D, Andreasson P, Meis-Kindblom JM, et al. Amplification of 12q13 and 12q15 sequences in a sclerosing epithelioid fibrosarcoma. *Cancer Genet Cytogenet*. 1998;107:102–106.
21. Ogose A, Kawashima H, Umezumi H, et al. Sclerosing epithelioid fibrosarcoma with der(10)t(10;17)(p11;q11). *Cancer Genet Cytogenet*. 2004;152:136–140.
22. Evans HL. Low-grade fibromyxoid sarcoma: a clinicopathologic study of 33 cases with long-term follow-up. *Am J Surg Pathol*. 2011;35:1450–1462.
23. Riggi N, Cironi L, Suva ML, et al. Sarcomas: genetics, signalling, and cellular origins. Part 1: The fellowship of TET. *J Pathol*. 2007;213:4–20.
24. Mitelman F, Johansson B, Mertens F. The impact of translocations and gene fusions on cancer causation. *Nat Rev Cancer*. 2007;7:233–245.
25. Bertolotti A, Melot T, Acker J, et al. EWS, but not EWS-FLI-1, is associated with both TFIID and RNA polymerase II: interactions between two members of the TET family, EWS and hTAFII68, and subunits of TFIID and RNA polymerase II complexes. *Mol Cell Biol*. 1998;18:1489–1497.
26. Bertolotti A, Lutz Y, Heard DJ, et al. hTAF(II)68, a novel RNA/ssDNA-binding protein with homology to the pro-oncoproteins TLS/FUS and EWS is associated with both TFIID and RNA polymerase II. *EMBO J*. 1996;15:5022–5031.
27. Lee J, Rhee BK, Bae GY, et al. Stimulation of Oct-4 activity by Ewing’s sarcoma protein. *Stem Cells*. 2005;23:738–751.
28. Powers CA, Mathur M, Raaka BM, et al. TLS (translocated-in-liposarcoma) is a high-affinity interactor for steroid, thyroid hormone, and retinoid receptors. *Mol Endocrinol*. 1998;12:4–18.
29. Rappaport J, Ryder U, Lamond AI, et al. Large-scale proteomic analysis of the human spliceosome. *Genome Res*. 2002;12:1231–1245.
30. Zhou Z, Licklider LJ, Gygi SP, et al. Comprehensive proteomic analysis of the human spliceosome. *Nature*. 2002;419:182–185.
31. Hicks GG, Singh N, Nashabi A, et al. Fus deficiency in mice results in defective B-lymphocyte development and activation, high levels of chromosomal instability and perinatal death. *Nat Genet*. 2000;24:175–179.
32. Kuroda M, Sok J, Webb L, et al. Male sterility and enhanced radiation sensitivity in TLS(-/-) mice. *EMBO J*. 2000;19:453–462.
33. Li H, Watford W, Li C, et al. Ewing sarcoma gene EWS is essential for meiosis and B lymphocyte development. *J Clin Invest*. 2007;117:1314–1323.
34. Fujii R, Takumi T. TLS facilitates transport of mRNA encoding an actin-stabilizing protein to dendritic spines. *J Cell Sci*. 2005;118:5755–5765.
35. Belly A, Moreau-Gachelin F, Sadoul R, et al. Delocalization of the multifunctional RNA splicing factor TLS/FUS in hippocampal neurones: exclusion from the nucleus and accumulation in dendritic granules and spine heads. *Neurosci Lett*. 2005;379:152–157.
36. Kwiatkowski TJ Jr, Bosco DA, Leclerc AL, et al. Mutations in the FUS/TLS gene on chromosome 16 cause familial amyotrophic lateral sclerosis. *Science*. 2009;323:1205–1208.
37. Vance C, Rogelj B, Hortobagyi T, et al. Mutations in FUS, an RNA processing protein, cause familial amyotrophic lateral sclerosis type 6. *Science*. 2009;323:1208–1211.
38. Kondo S, Hino SI, Saito A, et al. Activation of OASIS family, ER stress transducers, is dependent on its stabilization. *Cell Death Differ*. 2012;19:1939–1949.
39. Straessler KM, Jones KB, Hu H, et al. Modeling clear cell sarcomagenesis in the mouse: cell of origin differentiation state impacts tumor characteristics. *Cancer Cell*. 2013;23:215–227.